Rapid Communication

Removal of Ar$^+$ beam-induced damaged layers from polyimide surfaces with argon gas cluster ion beams

Takuya Miyayama,^{a*} Noriaki Sanada,^{a} Scott R. Bryan,^{b} John S. Hammond^b and Mineharu Suzuki^a

An Ar Gas Cluster Ion Beam (GCIB) has been shown to remove previous Ar$^+$ ion beam-induced surface damage to a bulk polyimide (PI) film. After removal of the damaged layer with a GCIB sputter source, XPS measurements show minor changes to the carbon, nitrogen and oxygen atomic concentrations relative to the original elemental bulk concentrations. The GCIB sputter depth profiles showed that there is a linear relationship between the Ar$^+$ ion beam voltage within the range from 0.5 to 4.0 keV and the dose of argon cluster ions required to remove the damaged layer. The rate of recovery of the original PI atomic composition as a function of GCIB sputtering is similar for carbon, nitrogen and oxygen, indicating that there was no preferential sputtering for these elements. The XPS chemical state analysis of the N 1s spectra after GCIB sputtering revealed a 17% damage ratio of altered nitrogen chemical state species. Further optimization of the GCIB sputtering conditions should lead to lower nitrogen damage ratios with the elemental concentrations closer to those of bulk PI. Copyright © 2010 John Wiley & Sons, Ltd.

Introduction

Ion sputter depth profiling (SDP) has been widely used with XPS, AES and SIMS for the characterization of thin film structures. Ion beam-induced damage during SDP is one of the key issues that must be understood in order to correctly interpret SDP results. A review article[1] published thirty years ago described physical atomic transport/displacement such as cascade mixing and diffusion as ion beam-induced damage during SDP. This review did not, however, discuss chemical damage. The review by Gillen et al.[2] discussed the applications of SF$_5^+$/F$^+$ and C$_n^+$/CsC$_n^-$ cluster ion beams to semiconductor and organic materials. Their data reports examples of secondary ion yield enhancement and minimal beam-induced degradation in SIMS and time-of-flight (TOF) SIMS SPD analyses. Wucher[3] also discussed secondary ion formation in TOF-SIMS analyses under cluster ion bombardment including C$_{60}^+$ and noted the benefits of secondary ion yield enhancement as well as the potential for non-destructive SPD of the chemical states for organic and biological materials.

Several publications have explored the benefits of using C$_{60}^+$ ion beams for SPD with XPS and TOF-SIMS for many materials.[3–15] One of the main benefits of C$_{60}^+$ sputtering reported in these publications is the reduction of chemical damage in the surface region during SPD. Chen et al.[4] used a C$_{60}^+$ ion beam for molecular SDP of trehalose films and reported that the degree of surface chemical damage accumulation was lower with C$_{60}^+$ than Au$_n^+$. Yamamoto[5] measured minimal changes in the XPS elemental compositions of soda-lime-silica glass with C$_{60}^+$ SDP. Weibel[6] also reported almost no damage with C$_{60}^+$ sputtering of polystyrene (PS) and polyethyleneterephthalate (PET). It has been reported that the amount of chemical damage from C$_{60}^+$ sputtering is strongly dependent on the incidence angle for PS and polycarbonate

(PC).[14] Yu et al.[9] reported the use of co-sputtering of C$_{60}^+$ and low energy monoatomic Ar$^+$ ions to achieve a constant sputter rate and a successful SDP of multiple organic thin films in a model organic light-emitting diode (OLED). It was suggested that success of the cosputtering technique was based on the Ar$^+$ ion beam breakage of crosslinking bonds in the organic film and the reduction of amorphous carbon depositing on the surface during the SPD. Recently, it has been reported that a gas cluster ion beam (GCIB) may be suitable as an alternative to monoatomic Ar$^+$ and C$_{60}^+$, for low damage SDP due to the sputtering process of such large cluster ions.[16]

Polyimide (PI) is a widely used industrial organic material because of its excellent thermal stability, insulating properties and mechanical flexibility. It is therefore highly desirable to analyze PI surface and thin film composition with XPS depth profiling to elucidate surface chemical modifications that affect its adhesion properties. Previous experiments using C$_{60}^+$ and coronene cluster ions have not been successful for obtaining a chemical SPD of a PI surface.[14] Attempts to use the cosputtering procedure[9] were also not successful with PI. In these experiments, the sputtered PI surfaces showed compositional damage with decreased nitrogen and oxygen atomic concentrations as well as a chemical degradation in the nitrogen bonding chemistry.

* Correspondence to: Takuya Miyayama, ULVAC-PHI, Inc., 370 Enzo, Chigasaki, Kanagawa, 253-8522, Japan. E-mail: takuya_miyayama@ulvac.com

a ULVAC-PHI, Inc., 370 Enzo, Chigasaki, Kanagawa, 253-8522, Japan

b Physical Electronics, Inc., 18725 Lake Drive East, Chanhassen, MN 55317, USA

In a recent study, low damage depth profiling of PI with XPS was demonstrated with an Ar GCIB source.[17] The GCIB sputtering resulted in much less chemical damage compared to the SDP results generated with $C_{60}{}^+$ and coronene cluster ion sources.

The degradation of the surface resulting from sputtering with low mass ions has been studied for some materials.[18–21] Shyue *et al.* has discussed the analysis of Si by XPS following cosputtering by atomic Ar^+ and $C_{60}{}^+$.[18] The ion beam-induced damage measured by cross-sectional transmission electron microscopy (X-TEM) and Rutherford backscattering spectroscopy (RBS) has been reported for GaN damaged by C, O, Si, Au and Bi ions,[19] for ZnO damaged by Si and Au ions,[20] and for Si damaged by Ga ions.[21] Although these publications have reported the thicknesses of the damaged layers, to date it has not been possible to remove the damaged layers and reveal a surface with its elemental and chemical structure equivalent to the materials before ion beam exposure.

In this report, GCIB sputtering is shown to successfully remove the Ar^+ ion-induced damaged layers and reveal a PI surface similar to the original PI composition and chemistry. The dose of GCIB sputtering to remove the Ar^+ ion beam-induced damaged layers as a function of the atomic Ar^+ ion beam energy is also reported.

Experimental

Commercial PI bulk films (Kapton HN, 0.125 mm thick, from Goodfellow Ltd) were used in this study. The C, N and O atomic concentrations in this PI film measured by an organic elemental analyzer were 76.25 ± 0.05 at.%, 6.40 ± 0.03 at.% and 17.35 ± 0.07 at.%, respectively. The SDP results were obtained with a PHI 5000 VersaProbe equipped with an Ar GCIB ion gun. The GCIB ion gun was operated at 10 keV beam energy (assuming single charged cluster ions) and 20 nA beam current. The angle of incidence of the GCIB was fixed at 55° from the sample normal, and the mean cluster size was around 2500 argon atoms/cluster (100 000 u). The GCIB was scanned over an area of 3 mm × 3 mm. The sputtering rate of the PI films under these conditions was approximately 1.0 nm/min, based on measuring the depth of a sputter crater produced in a fixed time with a mechanical stylus profiler. For XPS measurements, a monochromatic Al Kα (hν = 1486.6 eV) X-ray source with a beam diameter of 100 μm was focused at the sample surface. The measured photoelectron takeoff angle was 45° and the pass energy in the spherical capacitance analyzer (SCA) was fixed at 58.7 eV. The elemental surface concentrations of C, N and O were calculated from peak area measurements using appropriate elemental sensitivity factors. A simultaneous dual beam charge compensation technique with 1 eV electrons and 10 eV Ar^+ ions was used during XPS measurements. The damaged layers were formed on the PI sample surfaces with 0.5, 1.0, 2.0 and 4.0 keV energy Ar^+ ion beams. Each cycle consisted of Ar^+ irradiation of the PI surface to a dose of 2.0×10^{15} ions/cm^2 followed by XPS analyses. The total dose of Ar^+ ions was adjusted to 1.0×10^{16} ions/cm^2 for all beam energy conditions. Five cycles of Ar^+ ion irradiation followed by XPS analyses of the C 1s, O 1s and N 1s photoelectron spectra were acquired before the Ar GCIB SDP.

Results and Discussion

The compositional changes caused by Ar^+ ion irradiation as a function of ion dose (ions/cm^2) and GCIB SDP are shown in Fig. 1 for the Ar^+ ion beam energies of (a) 0.5, (b) 1.0, (c) 2.0 and (d) 4.0 keV.

All the results show a rapid decrease in oxygen and nitrogen and an increase in carbon atomic concentrations as a function of Ar^+ ion beam irradiation. The Ar^+ ion beam irradiation reduced the oxygen atomic concentrations to 5.2, 2.6, 1.6 and 1.1 at.% at beam energies of 0.5, 1.0, 2.0 and 4.0 keV, respectively, at a total ion dose of 1×10^{16} ions/cm^2. The C, O and N atomic concentrations changes induced by Ar^+ ion beam irradiation are summarized in Table 1. Ektessabi *et al.*[22] reported that higher Ar^+ ion beam energies lead to greater loss of oxygen concentration, consistent with the present results. Nitrogen concentrations also decrease from 4.7 at.% to 3.3 at.% as the Ar^+ ion beam energy was increased from 0.5 to 4.0 keV. The results shown in Fig. 1 demonstrate the successful use of a 10 keV Ar GCIB SDP to remove the Ar^+ ion beam-induced damage from a PI surface. The units of the abscissa are expressed as the Ar cluster dose as the sputtering rate for the damaged PI was not measured and may vary with the degree of damage. With continued GCIB sputter depth profiling, the XPS-measured atomic concentration values return to the values similar to bulk PI. The oxygen concentration on the surface after substantial Ar GCIB sputtering was approximately 14 at.% for all measurements. This value is 3 at.% smaller than the initial oxygen concentration of the PI film. This small difference is in significant contrast to the large decrease in oxygen concentration after irradiation with beams of Ar^+ (Table 1), $C_{60}{}^+$ and coronene ion species.[17] In the previous investigation,[17] a lower Ar GCIB energy was shown to decrease the loss of oxygen. The optimum match of XPS results with the bulk C, N and O PI atomic concentrations was achieved using a 2.5 keV Ar GCIB instead of the 10 keV Ar GCIB used in this study.

The chemical damage following Ar GCIB sputter depth profiling can be examined from the high-energy resolution XPS spectra. The N 1s spectra after Ar^+ ion beam irradiation show a peak with a binding energy of 399.3 eV[17] in addition to the N 1s peak at 400.6 eV binding energy of the original undamaged PI. The nitrogen damage ratio is defined as the peak area of the ion beam-induced damage component divided by the total N 1s peak area. Figure 2 shows the damaged and undamaged peak ratios for all of measured points in Fig. 1. The damage ratio increases to about 45% for 0.5 keV Ar^+ sputtering and up to 60% for 4 keV Ar^+ sputtering. Following 10 keV Ar GCIB sputtering the damage ratio decreased to about 17%.

The sputtering dose of the Ar GCIB to remove the Ar^+ beam-induced damaged layer and expose a surface composition similar to the original PI composition will be defined as the recovery dose. The recovery dose increases with higher Ar^+ ion beam energy as shown in Fig. 1. However, it should be noted that the N 1s spectra after the GCIB sputtering with a dose defined as the fully recovered dose show only 83% of the peak intensity consistent with the original PI N 1s peak position. The presence of the 17% damaged component is thought to be a limitation of using a 10 keV GCIB for this study.

The recovery dose is measured as the dose for an intensity increase or decrease of 16 to 84% or 84 to 16% for each element in these profiles. The recovery doses as a function of Ar^+ ion beam energy are plotted in Fig. 3. The recovery doses were obtained using a Logistic function[23] that is commonly used for quantitative interface analysis in SDP profiles. There is a linear relationship between the GCIB dose required to remove the damaged layer and the the Ar^+ ion beam energy. The plots for all three elements also show no recovery dose offset at the extrapolated value of zero Ar^+ ion beam energy. The similarity of the recovery doses of
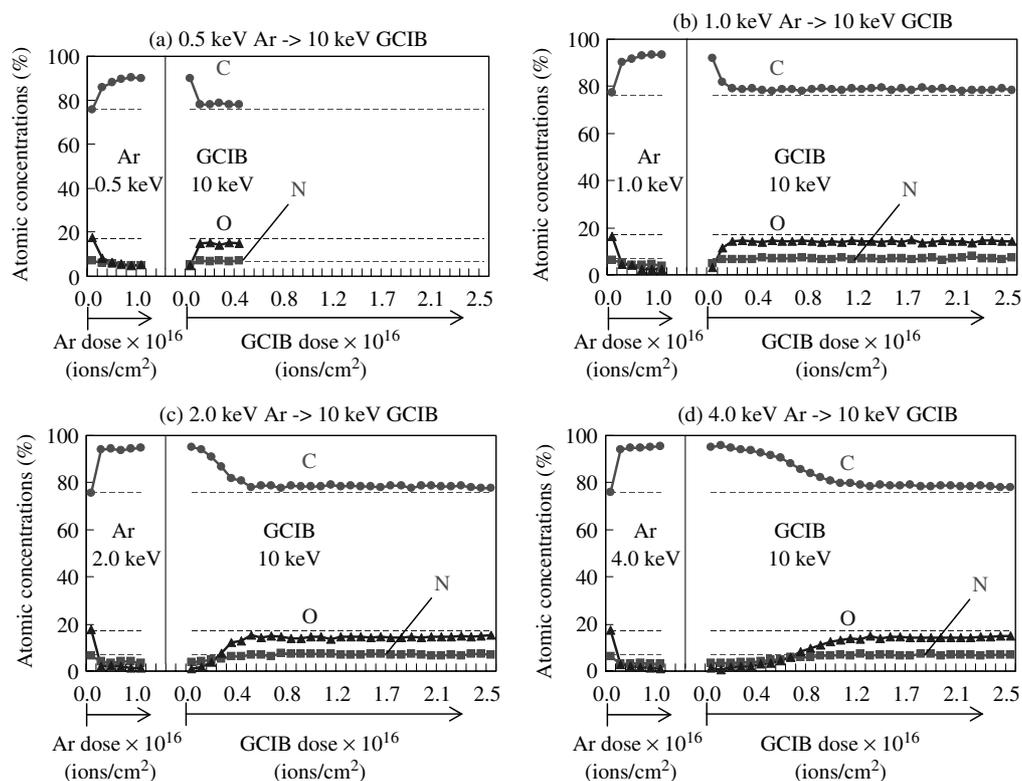
Figure 1. Ar^+ ion-induced damage and recovery of bulk elemental composition and chemistry with 10 keV Ar GCIB in PI films. The Ar^+ ion beam energies were: (a) 0.5 keV; (b) 1.0 keV; (c) 2.0 keV; and (d) 4.0 keV, respectively. The units of the abscissa are expressed as the dose of Ar cluster ions. The sputtering rate of undamaged PI is 1 nm/min for 10 keV Ar GCIB with the reported conditions. Note that the unmeasured sputtering rate of damaged PI may be significantly different than undamaged PI.

Table 1. Elemental concentration obtained by XPS after Ar^+ ion beam irradiation and organic elemental analysis. The total ion dose of Ar^+ at each energy was fixed at 1.0×10^{16} ions/cm²

Beam energy of Ar^+ (keV)	Atomic concentration (%)		
	C 1s	O 1s	N 1s
− *	76.25	17.35	6.40
0.5	90.1	5.2	4.7
1.0	93.5	2.6	3.9
2.0	94.9	1.6	3.6
4.0	95.6	1.1	3.3
* : Obtained with organic elemental analysis for the as-received film.			

all three elements at the same GCIB energy suggests that there is no observable preferential sputtering by the GCIB source.

Figure 4 shows the montage display of C 1s, O 1s and N 1s spectra acquired during GCIB SDP after 4.0 keV Ar^+ ion beam irradiation. The GCIB sputtering removes the damaged N 1s chemical component at 399.3 eV formed by Ar^+ ion irradiation, and the peak shape of N 1s becomes sharper with continued GCIB sputtering. For C 1s, there is only a broad peak shape at higher binding energies above the damaged C–C peak (284.3 eV binding energy) after Ar^+ ion beam irradiation. After GCIB sputtering, the C 1s peak shape clearly returns to the original PI peak shape with a prominent N–C=O peak at 288.7 eV binding energy. The O 1s peak shape also returns to the original PI O 1s peak shape with an appropriate $\pi - \pi^*$ shakeup structure after GCIB sputtering.

The results shown in Figs. 1–3 indicate that GCIB SDP can provide a means to profile a chemically altered surface of PI and expose the unaltered PI structure below the modified overlayer. It should be possible to obtain quantitative XPS analyses of buried structures by combining Ar^+ ion sputtering through the overlayer, followed by GCIB sputtering to remove the previous damaged chemistry.

In this report, the optimization of the Ar GCIB source conditions for SDP was not the primary focus, but this is very important for practical surface analyses. This report focused on the issue of removing surface damage introduced by an Ar^+ ion source for subsequent XPS SDP of a PI film. In the future, systematic studies should be performed to further optimize GCIB sputtering parameters such as ion incident angle, cluster size[24], impact energy and sample temperature, resulting in even smaller damage ratios. Lower damage cross-sections and lower damage accumulation have been reported for polymethylmethacrylate (PMMA) by decreasing the impact energy of SF_5^+ [25] and by decreasing the temperature,[26] respectively. Zemek *et al*.[27] reported that the surface roughness is smaller after Ar^+ irradiation than with Ar GCIB for PC. In this study, the surface roughening induced by GCIB irradiation was not investigated, but this will be studied in the near future similar to the previously reported atomic force microscopy (AFM) study of GCIB SDP applied to an organic multilayer system.[28] It is expected that GCIB depth profiling will significantly expand the applications for chemical depth profiling of polymers with surface analysis techniques such as XPS and TOF-SIMS.
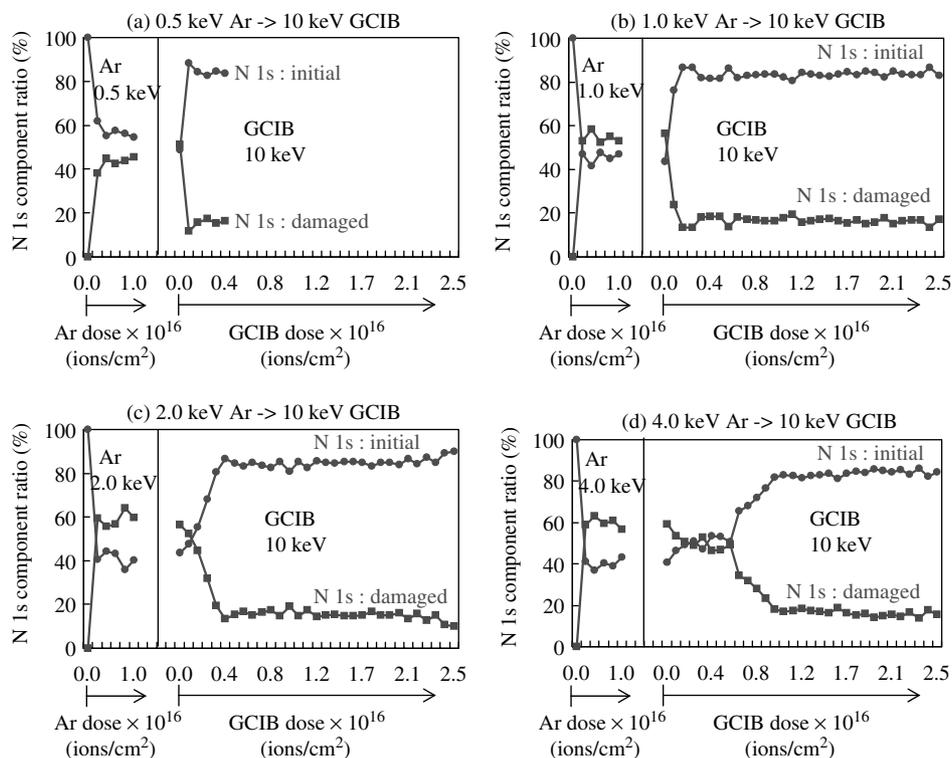
Figure 2. N 1s damage ratios vs Ar$^+$ ion dose and GCIB dose. The damage ratio is the peak area at 399.3 eV induced by Ar$^+$ ion sputtering divided by the total area of N 1s. The initial component ratio is the undamaged PI N 1s peak area divided by the total N 1s peak area, meaning that the sum of the initial and damaged N 1s components equal 100%. The units of the abscissa are expressed as the dose of Ar cluster ions. The sputtering rate of undamaged PI is 1 nm/min for 10 keV Ar GCIB with the reported conditions. Note that the unmeasured sputtering rate of damaged PI may be significantly different than undamaged PI.
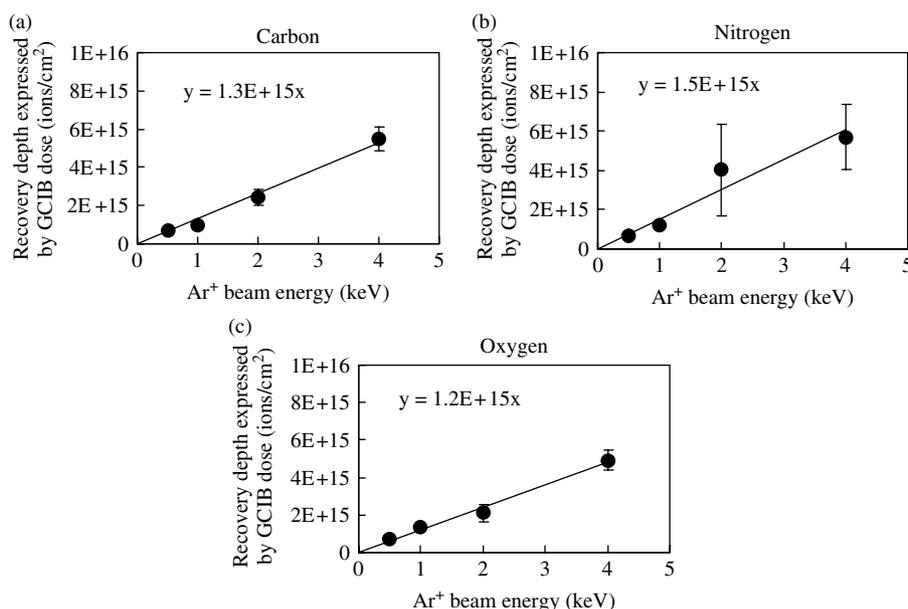

Figure 3. The relationship between the Ar$^+$ beam energy and recovery depth for: (a) carbon; (b) nitrogen; and (c) oxygen. The recovery depth is defined by intensity increase or decrease [16–84/84–16%] in the elemental profiles in Fig. 1. The linear functions are extrapolated through the origin. The units of the ordinate are expressed as the dose of Ar cluster ions. The sputtering rate of undamaged PI is 1 nm/min for 10 keV Ar GCIB with the reported conditions. Note that the unmeasured sputtering rate of damaged PI may be significantly different than undamaged PI.
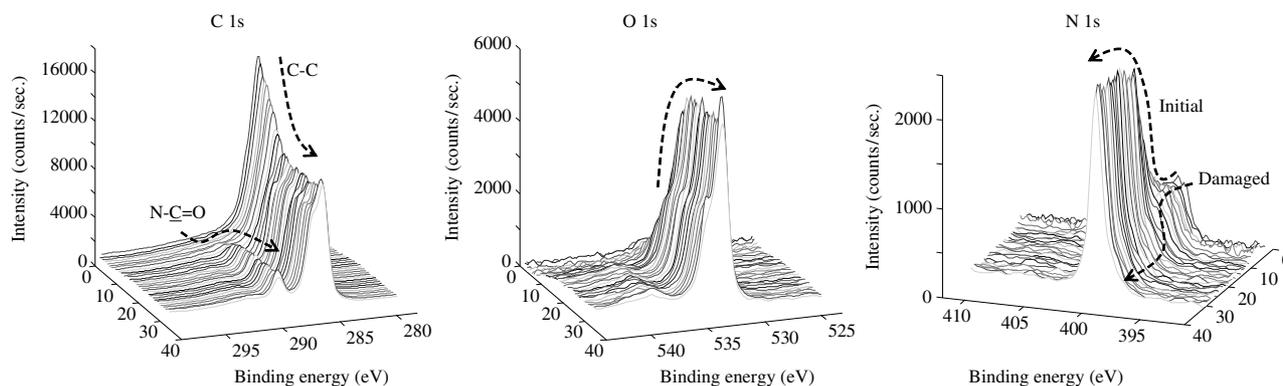
Figure 4. The montage displays of C 1s, O 1s and N 1s XPS spectra during GCIB dose profile acquired after 4.0 keV Ar$^+$ ion beam irradiation.

Conclusion

The removal of Ar$^+$ ion beam-induced damaged layers on the surface of PI and the return of elemental concentration and chemical spectroscopy measured by XPS similar to bulk PI films has been investigated with an Ar GCIB source. The PI surfaces exposed after GCIB sputtering show only small atomic % changes for carbon and oxygen from the undamaged elemental concentration. There is a linear relationship between the GCIB dose required to remove the Ar$^+$ ion beam-induced damaged layer and the Ar$^+$ ion beam energy in the range of 0.5–4.0 keV. Preferential sputtering by the GCIB source is not observed in the recovery of the bulk atomic concentration values of C, N, and O in the PI film. The XPS chemical spectroscopy shows similar spectra for the as received PI film and the PI film after removal of the damaged layer with the GCIB source. The small 17% damage ratio observed in the N 1s spectra after GCIB sputtering is minor compared to the extensive damage induced by sputtering with Ar$^+$, C$_{60}^+$ and coronene ions. Further optimization of the GCIB sputtering conditions could lead to elemental concentration numbers even closer to the bulk PI values and smaller N 1s damage ratios.

References

[1] S. M. Myers, *Nucl. Inst. Methods* **1980**, *168*, 265.
[2] G. Gillen, A. Fahey, *Appl. Surf. Sci.* **2003**, *203–204*, 209.
[3] A. Wucher, *Appl. Surf. Sci.* **2006**, *252*, 6482.
[4] J. Chen, A. Wucher, N. Winograd, *J. Phys. Chem. B.* **2006**, *110*, 8329.
[5] Y. Yamamoto, K. Yamamoto, *J. Non-Cryst. Solids* **2010**, *356*, 14.
[6] D. Weibel, S. Wong, N. Lockyer, P. Blenkinsopp, R. Hill, J. C. Vickerman, *Anal. Chem.* **2003**, *75*, 1754.
[7] K. Tanaka, N. Sanada, M. Hikita, T. Nkamura, T. Kajiyama, A. Takahara, *Appl. Surf. Sci.* **2008**, *254*, 5435.
[8] T. Nobuta, T. Ogawa, *Appl. Surf. Sci.* **2009**, *256*, 1560.
[9] B.-Y. Yu, Y.-Y. Chen, W.-B. Wang, M.-F. Hsu, S.-P. Tsai, W.-C. Lin, Y.-C. Lin, J.-H. Jou, C.-W. Chu, J.-J. Shyue, *Anal. Chem.* **2008**, *80*, 3412.
[10] J. Kozole, A. Wucher, N. Winograd, *Anal. Chem.* **2008**, *80*, 5293.
[11] A. G. Shard, F. M. Green, I. S. Gilmore, *Appl. Surf. Sci.* **2008**, *255*, 962.
[12] N. Sanada, A. Yamamoto, R. Oiwa, Y. Ohashi, *Surf. Interface Anal.* **2004**, *i*, 280.
[13] T. Miyayama, N. Sanada, S. Iida, J. S. Hammond, M. Suzuki, *Appl. Surf. Sci.* **2008**, *255*, 951.
[14] S. Iida, T. Miyayama, N. Sanada, M. Suzuki, G. L. Fisher, S. R. Bryan, *J. Surf. Sci. Nanotech.* **2009**, *7*, 878.
[15] G. L. Fisher, M. Dickinson, S. R. Bryan, J. Moulder. *Appl. Surf. Sci.* **2008**, *255*, 819.
[16] S. Ninomiya, Y. Nakata, K. Ichiki, T. Seki, T. Aoki, J. Matsuo. *Nucl. Instr. Meth. B.* **2007**, *256*, 493.
[17] T. Miyayama, N. Sanada, M. Suzuki, J. S. Hammond, S.-Q. D. Si, A. Takahara, *J. Vac. Sci. Technol. A.* **2010**, *28*, L1.
[18] B.-Y. Yu, W.-C. Lin, Y.-Y. Chen, Y.-C. Lin, K.-T. Wong, J.-J. Shyue, *Appl. Surf. Sci.* **2008**, *255*, 2490.
[19] S. O. Kucheyev, J. S. Williams, C. Jagadish, J. Zou, G. Li, A. I. Titov, *Phys. Rev. B.* **2001**, *64*, 35202.
[20] S. O. Kucheyev, J. S. Williams, C. Jagadish, J. Zou, C. E. Evans, A. J. Nelson, A. V. Hamza, *Phys. Rev. B.* **2003**, *67*, 94115.
[21] J. P. McCaffrey, M. W. Phaneuf, L. D. Madsen, *Ultramicroscopy* **2001**, *87*, 97.
[22] A. M. Ektessabi, S. Hakamata, *Thin Solid Films* **2000**, *377–378*, 621.
[23] LFPF (Logistic Function Profile Fitting program) from The National Institute of Standards and Technology, USA, http://www.cstl.nist.gov/div837/Division/outputs/LFPF/LFPF.htm [accessed: 15 July 2010].
[24] Y. Nakayama, S. Houzumi, N. Toyoda, K. Mochiji, T. Mitamura, I. Yamada, *Nucl. Instr. Meth. B.* **2005**, *241*, 618.
[25] M. S. Wagner, *Anal. Chem.* **2004**, *76*, 1264.
[26] C. M. Mahoney, A. J. Fahey, G. Gillen, *Anal. Chem.* **2007**, *79*, 828.
[27] J. Zemek, I. Yamada, G. Takaoka, J. Matsuo, *J. Vac. Sci. Technol. B.* **1999**, *17*, 2635.
[28] J. L. S. Lee, S. Ninomiya, J. Matsuo, I. S. Gilmore, M. P. Seah, A. G. Shard, *Anal. Chem.* **2010**, *82*, 98.